Chaotic flows in microchannels: A lattice Boltzmann Study

Max-Planck-Institut für Eisenforschung
Düsseldorf / Germany

F. Varnik, D. Raabe
varnik@mpie.de

Mikrostrukturphysik und Umformtechnik

Abstract

Roughness effects on lubricant flows are investigated via 2D lattice Boltzmann simulations. At a Reynolds number of 2500, a transition from laminar to unsteady flow is observed by an increase of the roughness height from about 4% to about 10% of the channel width. At a lower Reynolds number (where the flow is laminar in both the cases mentioned above), a transition toward flow instability may still be observed if the roughness height is increased further. The Reynolds number for the onset of flow instability thus decreases at higher wall roughness.

Our simulations also show that, in addition to the roughness height, a variation of the roughness *wave length* may also alter flow properties significantly. These observations underline the strong impact of the wall roughness on flow properties at moderate Reynolds numbers and in the case of strongly confined channels.

For a fixed Reynolds number and channel geometry, time and spatial dependence of the velocity field and fluctuating quantities obey the scaling behavior as expected from the structure of the Navier-Stokes (NS) equations, thus underlining the physical significance of our results.

Due to the ubiquitous presence of the wall roughness, the phenomenon is relevant in all cases where relatively high Reynolds number flow occur in strongly confined channels such as lubricant flow during the deformation of solid surfaces. Finally, a clever channel design allows a higher mixing efficiency without a variation of the Reynolds number.

Lattice Boltzmann simulations using experimental roughness data

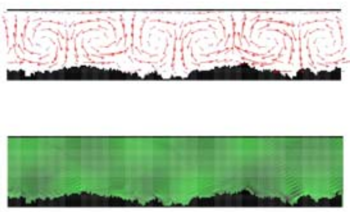

Fig. 1: Example (2D) of the application of a lattice Boltzmann fluid dynamics simulation to measured roughness data of plastically deformed iron. Velocity fluctuations (top) and the corresponding pressure distribution (bottom). The bright (dark) green corresponds to high (low) pressure. The channel dimensions are 10μm x 2μm.

Roughness wave length controls the transition towards instability

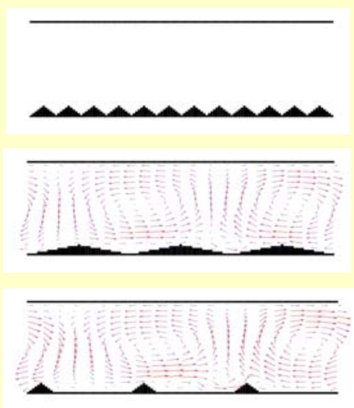

Fig. 2: The role of the roughness wave length, λ, on the transition toward flow instability. Velocity fluctuations are shown for three choices of wall roughness. While there are no fluctuations in the upper channel, they occur in the middle channel despite the fact that the roughness slope is reduced. Thus, λ plays a more important role than the roughness slope. The importance of roughness wave length is further examined in the bottom panel where λ is increased via obstacle removal (see also Fig. 7).

Roughness induced flow instability

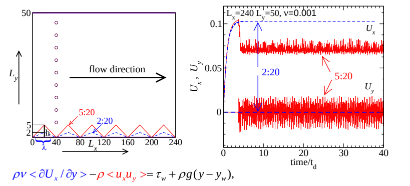

$\rho\nu < \partial U_x / \partial y > - \rho < u_x u_y > = \tau_w + \rho g (y - y_w)$,

where $u_x = U_x - < U_x >$, $u_y = U_y - < U_y >$,

g = external force and τ_w is the wall stress

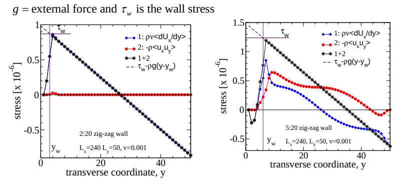

Fig. 3: Lattice Boltzmann simulations of roughness-induced flow instability. Here, the transition occurs via an increase of the roughness height. The two lower panels examine the validity of our simulations.

A further test of the results

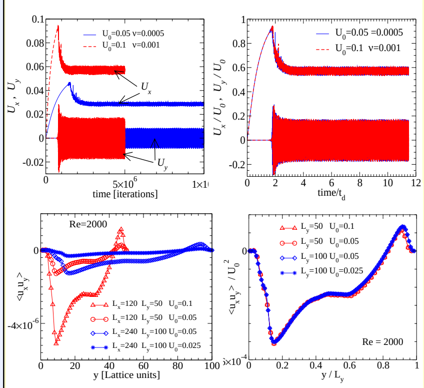

Fig. 4: Top: Fluid velocity in the channel center versus time for two values of the characteristic velocity. Bottom: The Reynolds stress for two channel widths and two characteristic flow velocities. All curves shown in the left panels obey the same master curve if the simulated data are expressed in units of the characteristic length and the characteristic flow velocity. In all the cases shown above, both the Reynolds number and the channel shape are kept constant.

Stamping experiment: Relevant Reynolds numbers

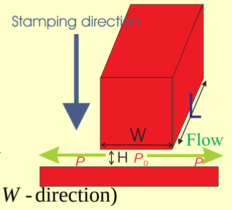

For $L >> W$: $\frac{p - p_0}{L} << \frac{p - p_0}{W}$

(higher pressure gradient in the W - direction)

$\rightarrow$ Main flow in the W - direction

It follows from the incompressibility condition :

$$0 = \frac{\dot{V}}{V} = \frac{\dot{L}}{L} + \frac{\dot{W}}{W} + \frac{\dot{H}}{H}$$

schematic view of the contact region:

$$\Rightarrow \dot{W} = -\frac{W}{H}\dot{H} \text{ (using } \dot{L} = 0)$$

$$\Rightarrow \mathrm{Re} = \left|\frac{\dot{W} H}{\nu}\right| = \left|\frac{W \dot{H}}{\nu}\right| \text{ (indep. of H!)}$$

$\dot{H} \in [10^{-4} ... 10^{-1}]$m/s, $\nu = 10^{-5}$m^2/s, $W = 10^{-1}$m

$\Rightarrow \mathrm{Re} \in [1...1000]$

→ Inertial effects not negligible!

Surface roughness measurements

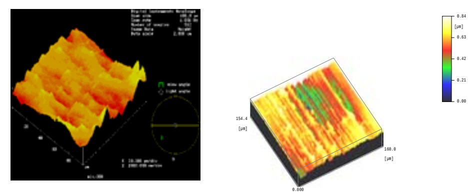

Fig. 5: Experimentally determined surface roughnesses as measured via atomic force microscopy (left) and confocal microscopy (right) of metallic sheets.

Impact of flow on plastic deformation

Fig. 6: Results of stamping experiments with (top) and without (bottom) lubricant flow.

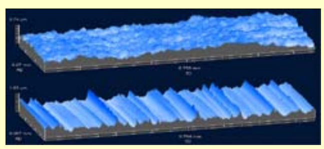

A simple way to considerably enhance the mixing efficiency

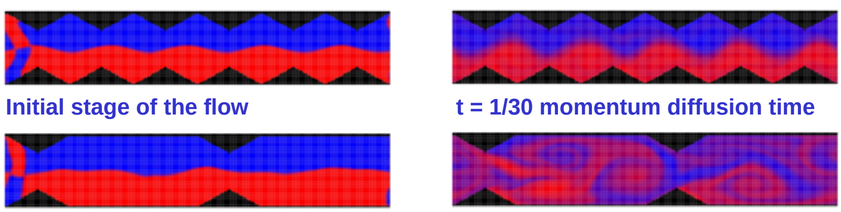

Fig. 7: Dispersion of a passive tracer (red color) under flow. The Reynolds number is identical for both channels (Re=1500). A transition from a quasi laminar flow to a fully chaotic one takes place as the roughness wave length is increased by removal of obstacles (see also Fig. 2).

References:

Our Work

F. Varnik and D. Raabe, *Modelling Simul. Mater. Sci. Eng.* (submitted); F. Varnik and D. Raabe, *J. Fluid Mech.* (submitted) ; D. Raabe, *Modelling Simul. Mater. Sci. Eng.* **12**, R 13 (2004).

Monographs on the Lattice Boltzmann Method

S. Succi, *The Lattice Boltzmann Equation for Fluid Dynamics and Beyond*; D.H. Rothman, S. Zaleski, *Lattice-Gas Cellular Automata;* D. Wolf-Gladrow, *Lattice-Gas Cellular Automata and Lattice Boltzmann Models.*

Papers on Chaotic Mixing

C. Simonnet, A. Groisman, *Phys. Rev. Lett.* **94**, 134501 (2005); A.D. Strook et al., *Science* **295**, 647 (2002); M.C. Jullien, P. Castiglione and P. Tabeling, *Phys. Rev. Lett.* **85**, 3636 (2000); R.A. Truesdell et al., *Phys. Rev. E* **67** 066304 (2003).